

## Reduction of N<sub>2</sub>O with Hydrosilanes Catalysed by RuSNS Nanoparticles

Pablo Molinillo,<sup>a</sup> Bertrand Lacroix,<sup>b,c</sup> Florencia Vattier,<sup>d</sup> Nuria Rendón,<sup>\*a</sup> Andrés Suárez<sup>\*a</sup> and Patricia Lara<sup>\*a</sup>

<sup>a</sup>*Instituto de Investigaciones Químicas (IIQ), Departamento de Química Inorgánica, and Centro de Innovación en Química Avanzada (ORFEO-CINQA), CSIC and Universidad de Sevilla. Avda. Américo Vespucio 49, 41092 Sevilla, Spain.*

<sup>b</sup>*Department of Material Science and Metallurgic Engineering, and Inorganic Chemistry, University of Cádiz, Spain.*

<sup>c</sup>*IMEYMAT: Institute of Research on Electron Microscopy and Materials of the University of Cádiz, Spain.*

<sup>d</sup>*Instituto de Ciencia de Materiales de Sevilla, CSIC-Universidad de Sevilla, Avda. Américo Vespucio 49, 41092 Sevilla, Spain.*

**Table of contents:**

**S1. General, materials and characterization techniques.**

**S2. Synthesis of ruthenium nanoparticles.**

**S3. TEM and HRTEM/EDX images.**

**S4. Representative procedure for Reduction of N<sub>2</sub>O with Hydrosilanes.**

**S5. Representative procedure for control experiments. H<sub>2</sub> detection, mercury test and [Ru(COD)(COT)] catalysis.**

**S6. NMR and HRMS data for catalytic reactions products.**

**S7. References.**

## S1. General, materials and characterization techniques.

All operations were carried out using standard Schlenk tubes, Fisher-Porter bottle techniques or in a glove box under nitrogen atmosphere. Solvents were distilled under nitrogen with the following desiccants: sodium benzophenone-ketyl for tetrahydrofuran (THF), and sodium for pentane. SNS ligands were synthesized using previously reported methods.<sup>1</sup> [Ru(COD)(COT)] was prepared as previously reported.<sup>2</sup> H<sub>2</sub> (99.99%) was purchased from Air Liquide. Dimethylphenethylsilane was prepared following a literature procedure.<sup>3</sup> All the other reactants were used as received from the commercial supplier (Aldrich).

The size, structure and composition of Ru·L NPs were studied by transmission electron microscopy (TEM) in a Philips CM200 or FEI TALOS F200S working at 200kV at the “Centro de Investigación, Tecnología e Innovación – CITIUS” (University of Sevilla). Prior to TEM experiments, a drop of the crude THF colloidal solution or a drop of a solution of the isolated and purified nanoparticles after dispersion in THF was deposited on a covered holey copper grid. The approximation of the particles mean size was made through a manual analysis of enlarged conventional TEM micrographs by measuring *ca.* 300 particles on a given grid. The Ru·L NPs crystal structure was analyzed from high-resolution TEM (HRTEM) images using Digital Micrograph. An ABSF filter available within the “HRTEM filter” plugin was applied to enhance contrast by reducing the noise due to surrounding amorphous materials.<sup>4</sup> STEM-EDX spectrum images using scanning TEM mode combined with energy-dispersive X-ray spectrometry, were acquired over various NPs to assess their composition. A small electron probe (size ~0.5 nm, current ~500 pA) was scanned over an area of 140x160 pixels with a dwell time of 50 μs/pixel and the EDX signal was integrated over about 200 frames using drift correction. The high-angle annular dark-field (HAADF) signal was also recorded simultaneously to locate the NPs. Net integrated intensity maps of the Ru-L line were then extracted after applying a set of pre- and post-filtering functions using the Velox software.

Liquid phase <sup>1</sup>H NMR spectra were recorded on Bruker DRX-500, DRX-400 spectrometers. Spectra were referenced to external SiMe<sub>4</sub> (δ = 0 ppm) using the residual protio solvent peaks as internal standards.

ICP analyses were performed at “Mikroanalytisches Labor Pascher” (Remagen, Germany).

X-Ray photoelectron spectroscopy (XPS) experiments were performed in a PHOIBOS-100 spectrometer with a nonmonochromatic Mg-Kα radiation ( $h\nu = 1235.6$  eV) and the power source was 230 W. The electron energy hemispherical analyzer was operated in the constant pass energy mode (SPECS PHOIBOS 100DLD). Low resolution survey spectra were obtained with a pass energy = 50 eV, while high energy resolution spectra of detected elements (*i.e.*, Ru3p, N1s, S2p) were obtained with a pass energy = 35 eV. The spectra were analyzed with the “CASA XPS” software, version 2.3.16.Dev52 (Neal Fairly, UK). Shirley type backgrounds were used to determine the areas under

the peaks. The Ru3p<sub>3/2</sub> spectra were fitted with two components, corresponding to Ru(0) and Ru(IV), using Gaussian-Lorentzian functions (GL = 30). Samples were prepared by absorption of a solution of nanoparticles into a piece of filter paper (1 cm<sup>2</sup>), then allowed to evaporate in an inert atmosphere inside a glove box to minimize surface contamination. The samples were transferred to the spectrometer under inert atmosphere and the measurements were made with a constant pressure in the analyser chamber of 10<sup>-9</sup> torr. This procedure allows to maintain the stability of the nanoparticles by preventing their agglomeration; however, the presence of C and O in the matrix used makes it difficult to unequivocally characterize these elements in the studied nanoparticles. Due to the presence of carbon atoms in the different ligands and in the cellulose matrix, it was not possible to use the adventitious carbon contamination for the binding energy shift calibration. Instead, the constant presence of silicon atoms from the vacuum grease provides us a good reference in all the spectra (Si2p signal at 102.4 eV in B.E.).<sup>5</sup>

HRMS experiments were carried out in a Thermo Scientific-QExactive apparatus by the Mass Spectrometry Service of the “Centro de Investigación, Tecnología e Innovación – CITIUS” (University of Sevilla).

GC-MS analysis of the catalytic reactions headspaces were carried out using a Shimadzu GCMS-TQ8040 apparatus equipped with a PoraBOND Q capillary column (25 m, 0.25 mm i.d., 3 μm film thickness). Helium carrier gas was supplied at a head pressure of 3.7 psi to provide an initial flow rate of 4.6 mL/min. The injector temperature was setup to 200 °C, and the oven temperature was initially held at 30 °C for 5 min, then gradually increased to 150 °C at 25 °C/min. Full-scan mass spectra were collected from *m/z* 10 to 50 at a data acquisition rate of 158 spectra/s. The MS transfer line was held at 250 °C and the ion source temperature was 200 °C.

## **S2. Synthesis of ruthenium nanoparticles.**

[Ru(COD)(COT)] (200 mg, 0.64 mmol) was introduced in a Fisher-Porter bottle and dissolved in 50 mL of freshly distilled and degassed THF by N<sub>2</sub> bubbling. The resulting yellow solution was cooled to -50 °C, and 20 mL of a THF solution containing the SNS ligand (0.32 mmol for Ru·L1<sup>0.5</sup>, Ru·L2<sup>0.5</sup>, Ru·L3<sup>0.5</sup> and Ru·L4<sup>0.5</sup>; 0.13 mmol for Ru·L4<sup>0.2</sup>) was added into the reactor. The Fisher-Porter bottle was pressurized with 3 bar of H<sub>2</sub> and the solution was left to reach slowly the room temperature under vigorous stirring. The homogenous solution, which turns black after 30 minutes of reaction, was kept under stirring overnight at room temperature. After this period of time, excess of H<sub>2</sub> was carefully released, and the volume of solvent was reduced to 10 mL under vacuum. 30 mL of pentane were then added to the colloidal suspension which was cooled down to -30°C to precipitate the particles. After filtration under argon with a cannula, the black solid powder was washed three times with pentane (3 × 40 mL), and filtrated again before drying under vacuum.

### **Sample Ru·L1<sup>0.5</sup>**

Ru content (ICP): 41%

TEM: NPs of 1.5 (0.2) nm mean size

Yield: 52 mg.

### **Sample Ru·L2<sup>0.5</sup>**

Ru content (ICP): 32%

TEM: NPs of 1.9 (0.4) nm mean size

Yield: 80 mg.

### **Sample Ru·L3<sup>0.5</sup>**

Ru content (ICP): 41%

TEM: NPs of 1.5 (0.2) nm mean size

Yield: 50 mg.

### **Sample Ru·L4<sup>0.5</sup>**

Ru content (ICP): 47%

TEM: NPs of 1.6 (0.2) nm mean size

Yield: 60 mg.

### Sample Ru·L4<sup>0.2</sup>

Ru content (ICP): 81%

TEM: NPs of 2.3 (0.4) nm mean size

Yield: 65 mg.

### S3. TEM and HRTEM/EDX images.

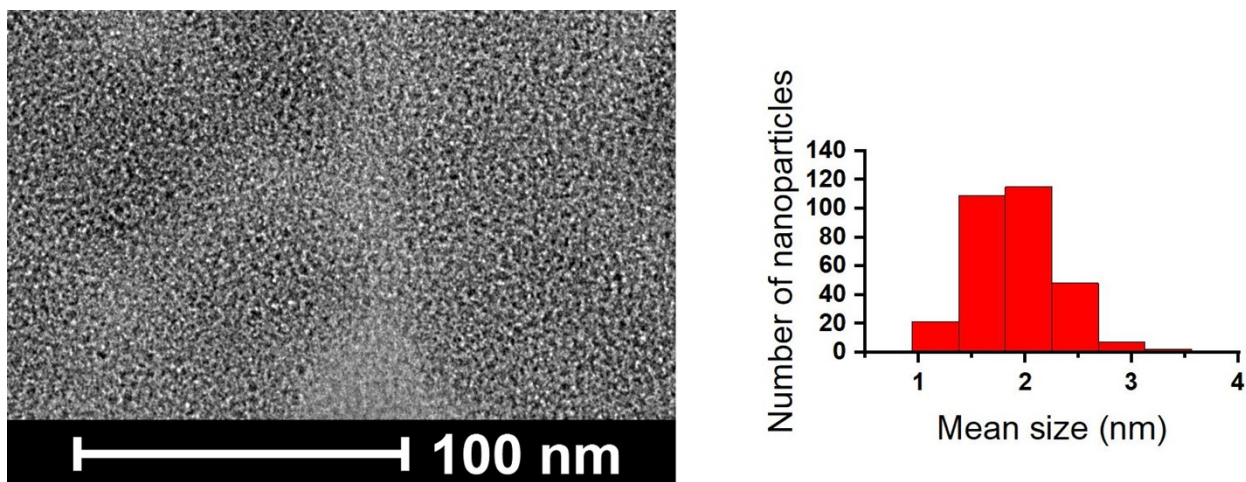


Figure S1. TEM image of Ru·L2<sup>0.5</sup> nanoparticles.

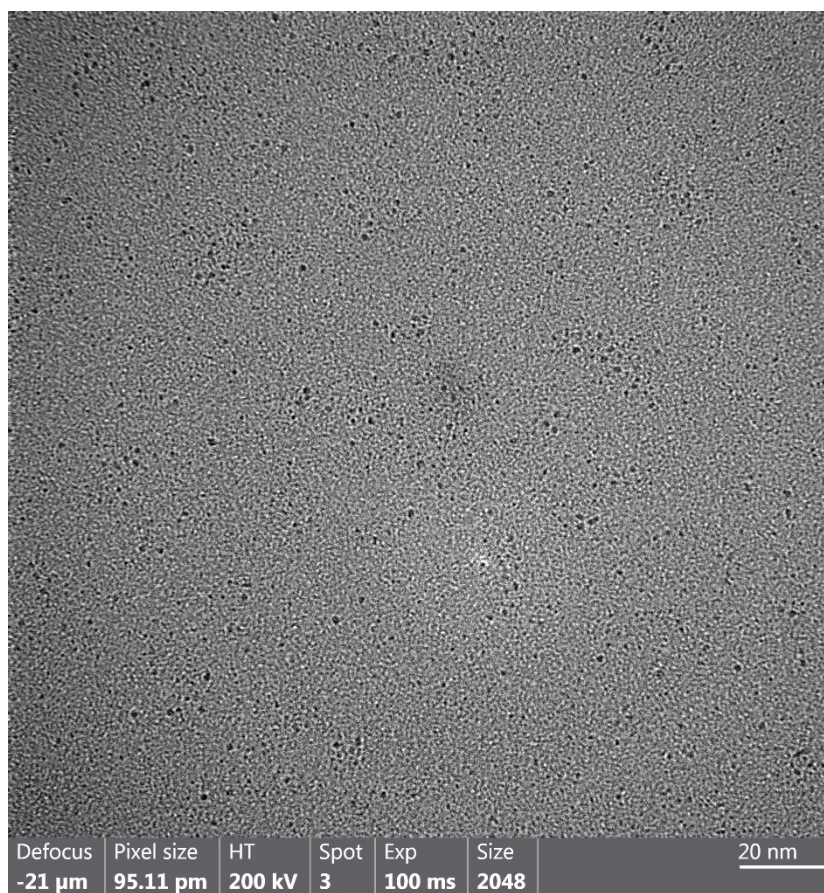
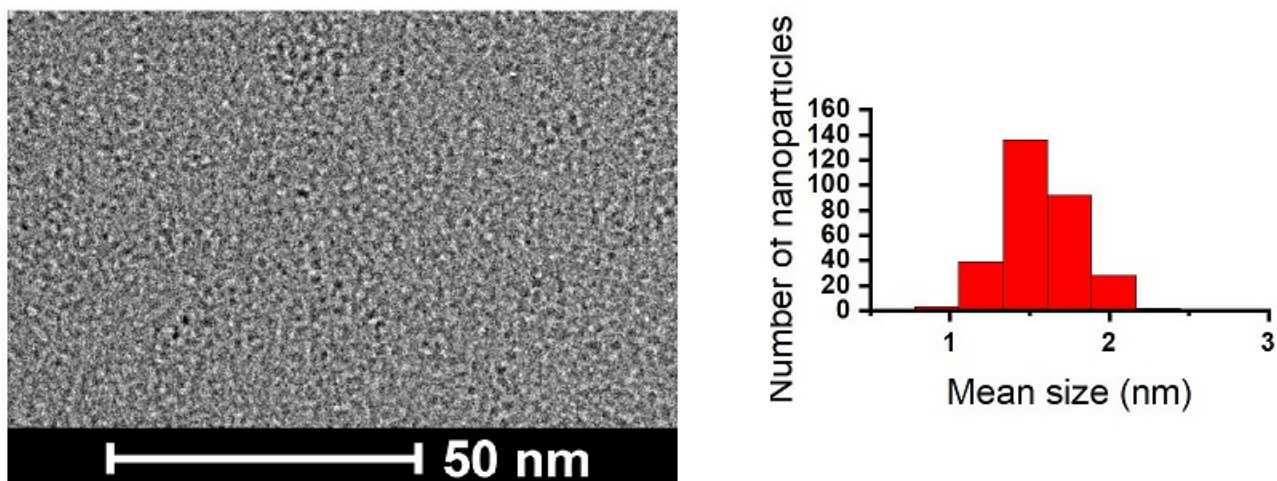
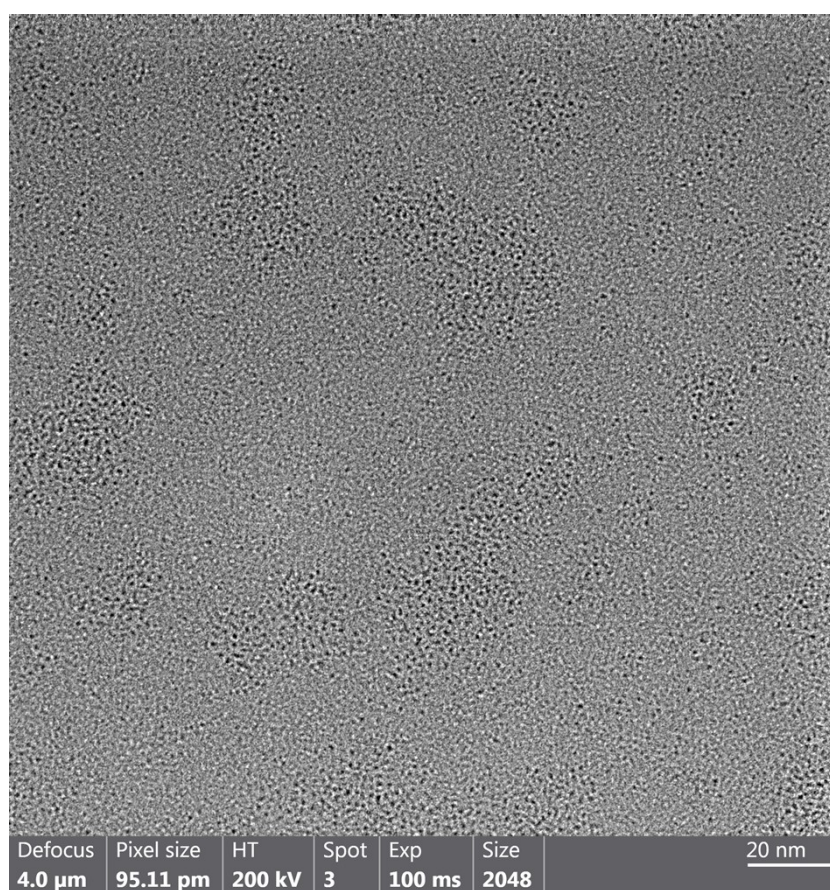


Figure S2. TEM image of Ru·L2<sup>0.5</sup> nanoparticles at higher magnification.



**Figure S3.** TEM image of Ru·L3<sup>0.5</sup> nanoparticles.



**Figure S4.** TEM image of Ru·L3<sup>0.5</sup> nanoparticles at higher magnification.

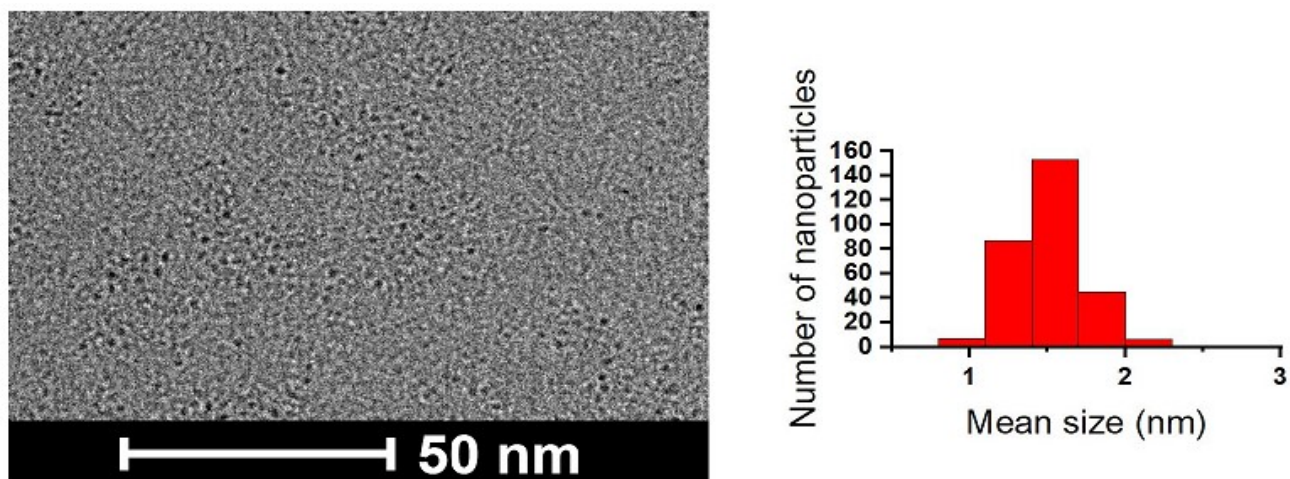


**Figure S5.** TEM image of Ru·L4<sup>0.5</sup> nanoparticles.

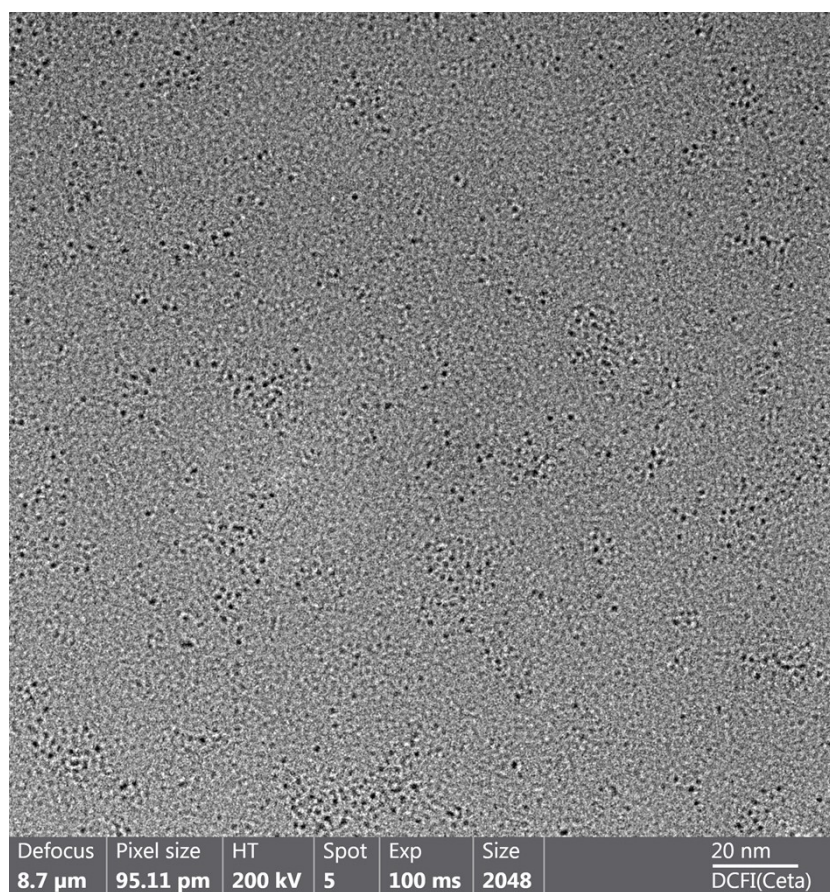


**Figure S6.** TEM image of Ru·L4<sup>0.5</sup> nanoparticles at higher magnification.

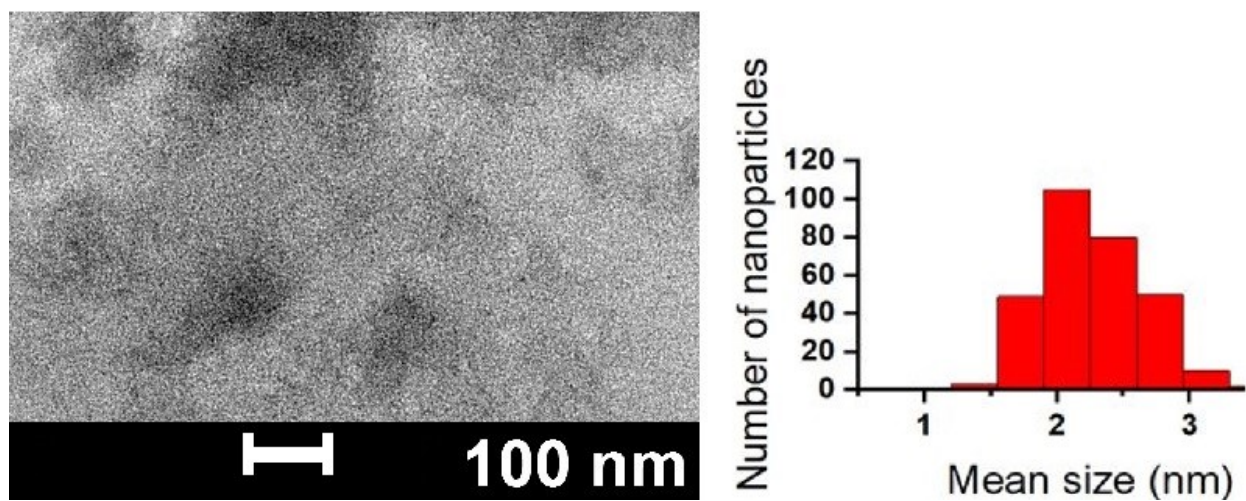


**Figure S7.** TEM image of Ru·L4<sup>0.2</sup> nanoparticles.



**Figure S8.** TEM image of Ru·L4<sup>0.2</sup> nanoparticles at higher magnification.

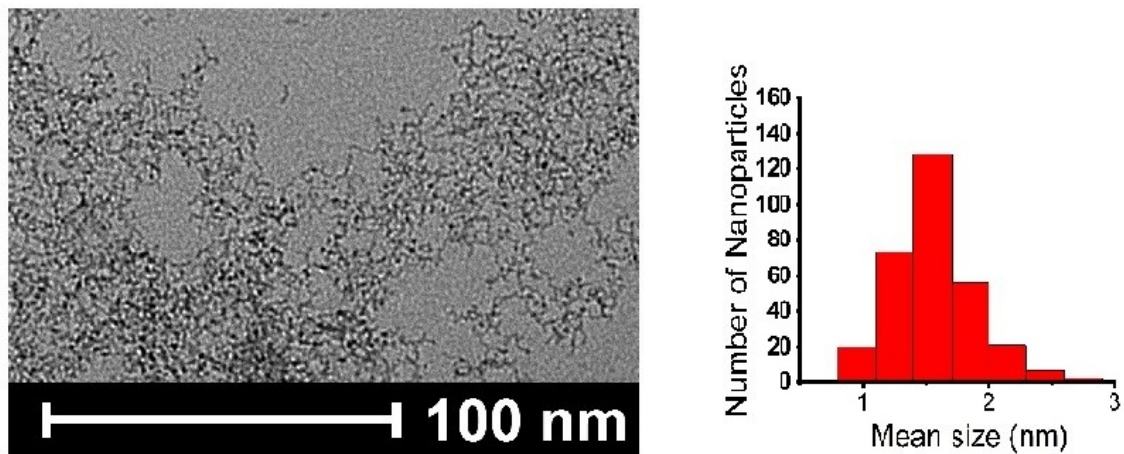
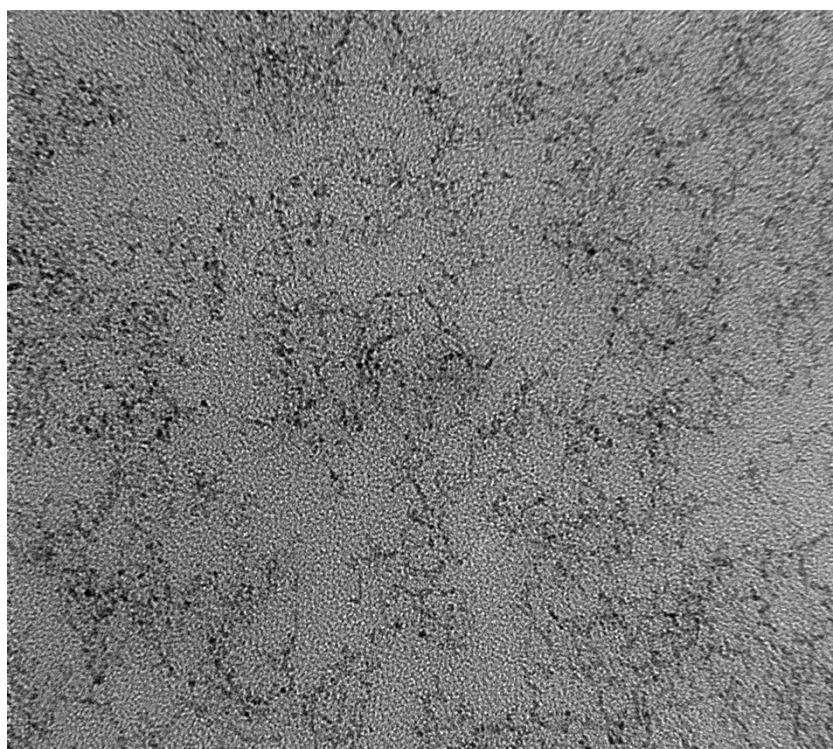
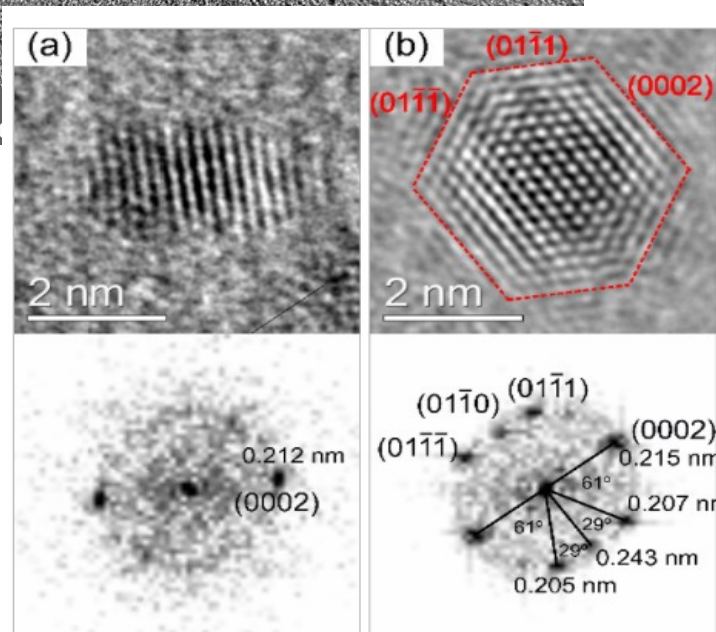


**Figure S9.** TEM image of Ru-L4<sup>0.5</sup> nanoparticles after catalytic reaction (Table 2, entry 5).



Defocus	Pixel size	HT
4.9 nm	95.11 $\mu$ m	200

**Figure S10.**  
Ru-L4<sup>0.5</sup>  
catalytic reaction  
magnification



TEM image of  
nanoparticles after  
at higher  
(Table 2, entry 5).

**Figure S11.** HRTEM images (up) and FFT pictures (down) obtained for Ru·L2<sup>0.5</sup> nanoparticles.

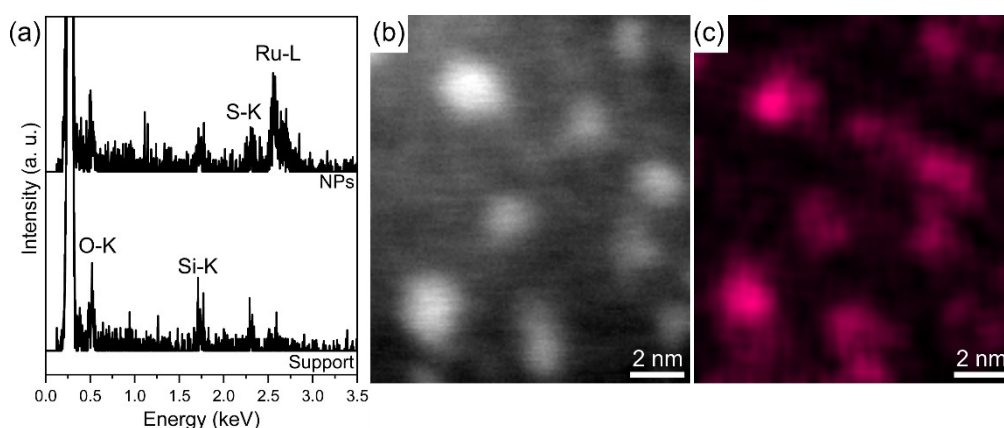


**Figure S12.** EDX spectra (a), STEM-HAADF image (b) and Ru-L intensity map (c) obtained for Ru·L2<sup>0.5</sup> nanoparticles.

#### S4. Representative procedure for hydrosilylation of N<sub>2</sub>O.

In a glovebox, a Fisher–Porter vessel (25 mL) was charged with a solution of dimethylphenylsilane (115  $\mu$ L, 0.75 mmol) in THF (0.2 mL) and 0.3 mL of a freshly prepared stock suspension of colloidal catalyst Ru·L4<sup>0.5</sup> (7.5  $\mu$ mol Ru). The nitrogen atmosphere in the reactor was replaced by 1 bar of N<sub>2</sub>O by performing three freeze-pump-thaw cycles and heated to 55  $^{\circ}$ C. After 24 h, the gas atmosphere was analysed by GC-MS to detect N<sub>2</sub> formation (Figure S8). The reactor was depressurized, and an aliquot of the reaction mixture was filtered through a short pad of celite and analyzed by GC-MS and <sup>1</sup>H NMR spectroscopy. To further confirm the identity of the reaction

products, these were isolated using flash chromatography on silica gel (eluent: pentane → pentane/Et<sub>2</sub>O, 1:1).

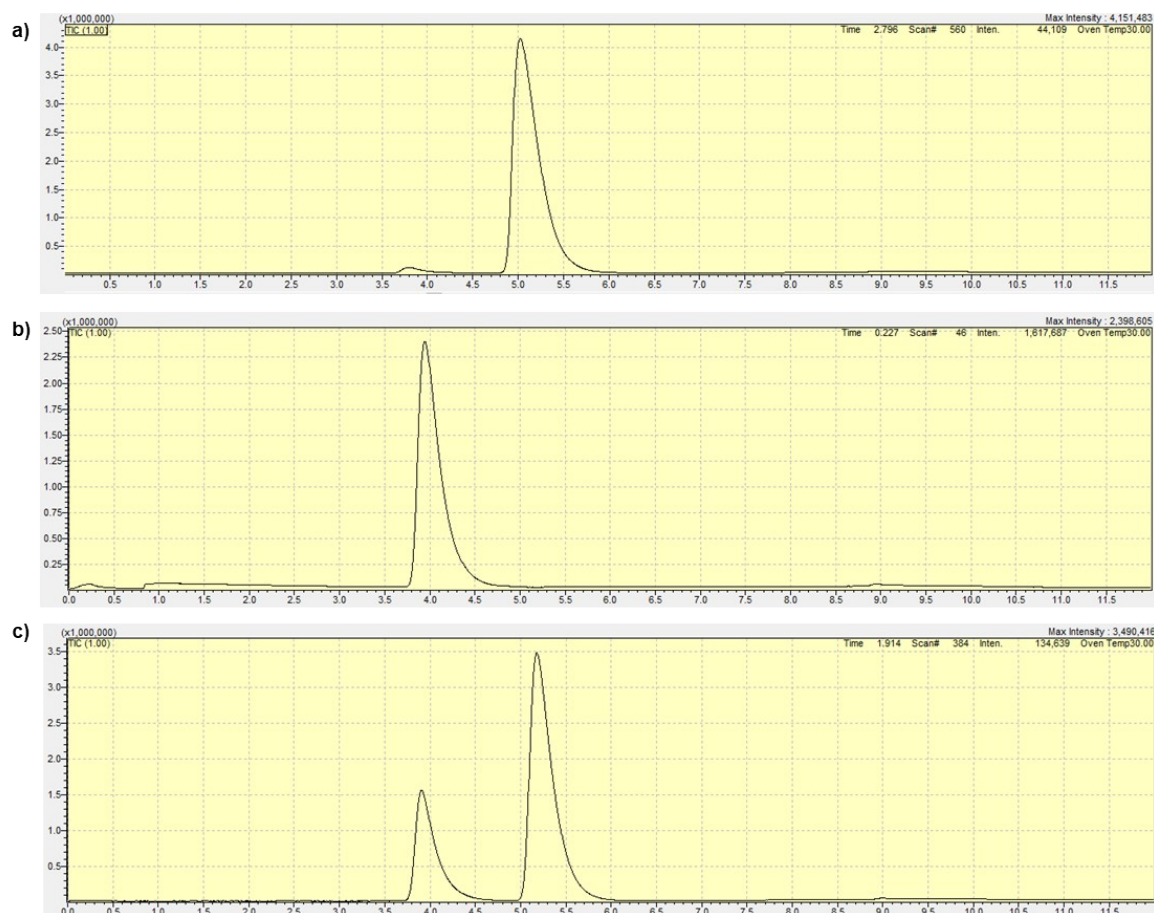


**Figure S13.** N<sub>2</sub> determination by GC-MS: a) control experiment N<sub>2</sub>O; b) control experiment N<sub>2</sub>; c) catalytic reaction (Table 3, entry 1).

## S5. Representative procedure for control experiments. H<sub>2</sub> detection, mercury test and [Ru(COD)(COT)] catalysis.

### H<sub>2</sub> detection

In a glovebox, a pressure RMN-tube was charged with a solution of dimethylphenylsilane (115  $\mu$ L, 0.75 mmol) in THF-d<sub>8</sub> (0.1 mL) and 0.2 mL of a freshly prepared suspension of colloidal catalyst Ru·L<sup>4</sup><sub>0.5</sub> (7.5  $\mu$ mol Ru) in THF-d<sub>8</sub>. In addition to that, another THF-d<sub>8</sub> (0.2 mL) solution of dimethylphenylsilanol (123  $\mu$ L, 0.75 mmol) was also added to the tube, which was heated to 55°C. After 24 h, the reaction was studied by <sup>1</sup>H NMR spectroscopy, which revealed the formation of (Me<sub>2</sub>PhSi)<sub>2</sub>O along with H<sub>2</sub> ( $\delta$ 4.5 ppm).

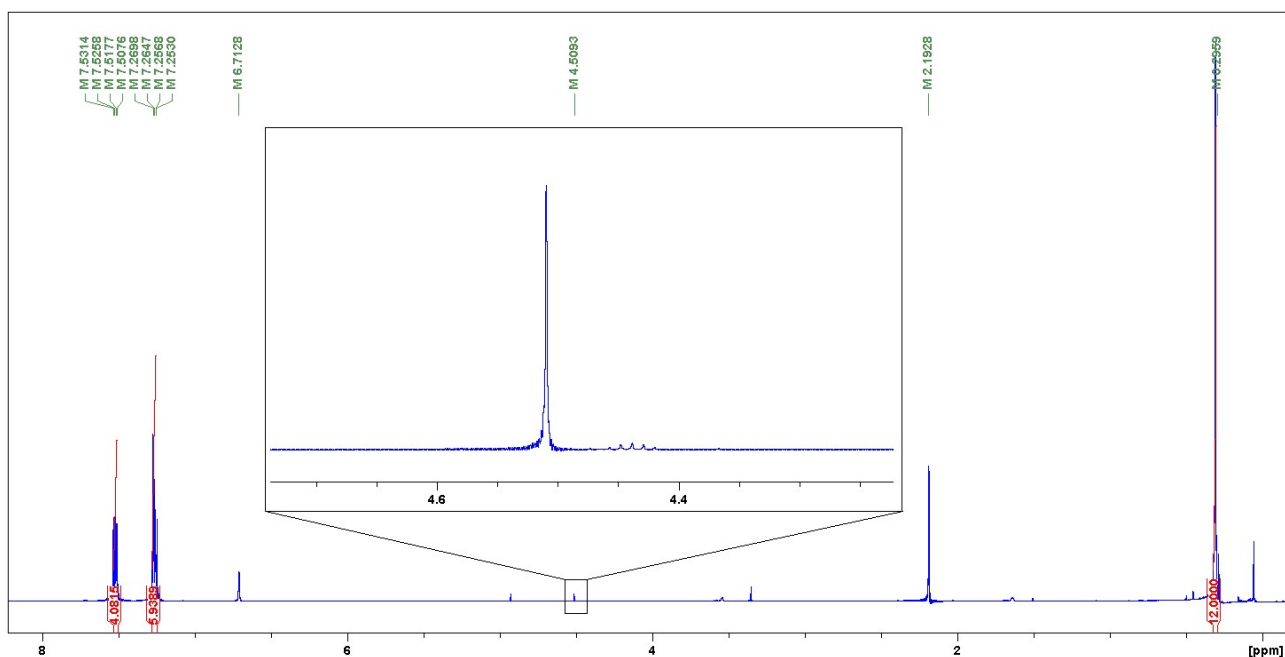


**Figure S14.**  $^1\text{H}$  NMR spectrum (THF- $d_8$ , 400 MHz) of control experiment for detection of  $\text{H}_2$ .

### Mercury test.

The test was carried out according to the general procedure specified at S4, adding Hg (20 mg, 0.1 mmol) to the reaction mixture. In this case, the conversion decreases from >99% (see table 2, entry 5) to 45%, that may suggest two different mechanisms acting simultaneously (homogeneous/colloidal).

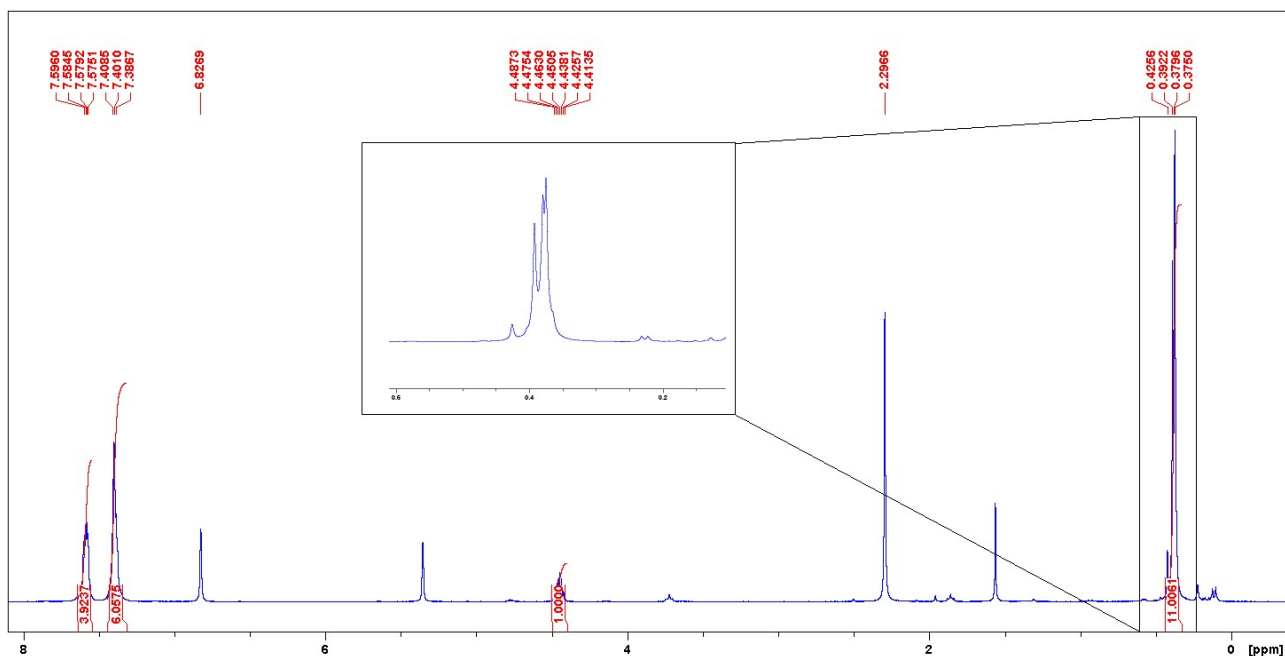


**Figure S15.**  $^1\text{H}$  NMR spectrum ( $\text{CD}_2\text{Cl}_2$ , 300 MHz) of catalysis in presence of Hg.

### [Ru(COD)(COT)] catalysis

In a glovebox, a Fisher–Porter vessel (25 mL) was charged with a THF (0.2 mL) solution of dimethylphenylsilane (115  $\mu$ L, 0.75 mmol) and 0.3 mL of a freshly prepared suspension of [Ru(COD)(COT)] (7.5  $\mu$ mol Ru) in THF. The nitrogen atmosphere in the reactor was replaced by 1 bar of N<sub>2</sub>O by performing three freeze-pump-thaw cycles and the reaction was heated at 55 °C for 24h. The reactor was depressurized, and an aliquot of the reaction mixture was filtered through a short pad of celite and analyzed by <sup>1</sup>H NMR spectroscopy. The <sup>1</sup>H NMR spectrum reveals a conversion lower than 5 %.

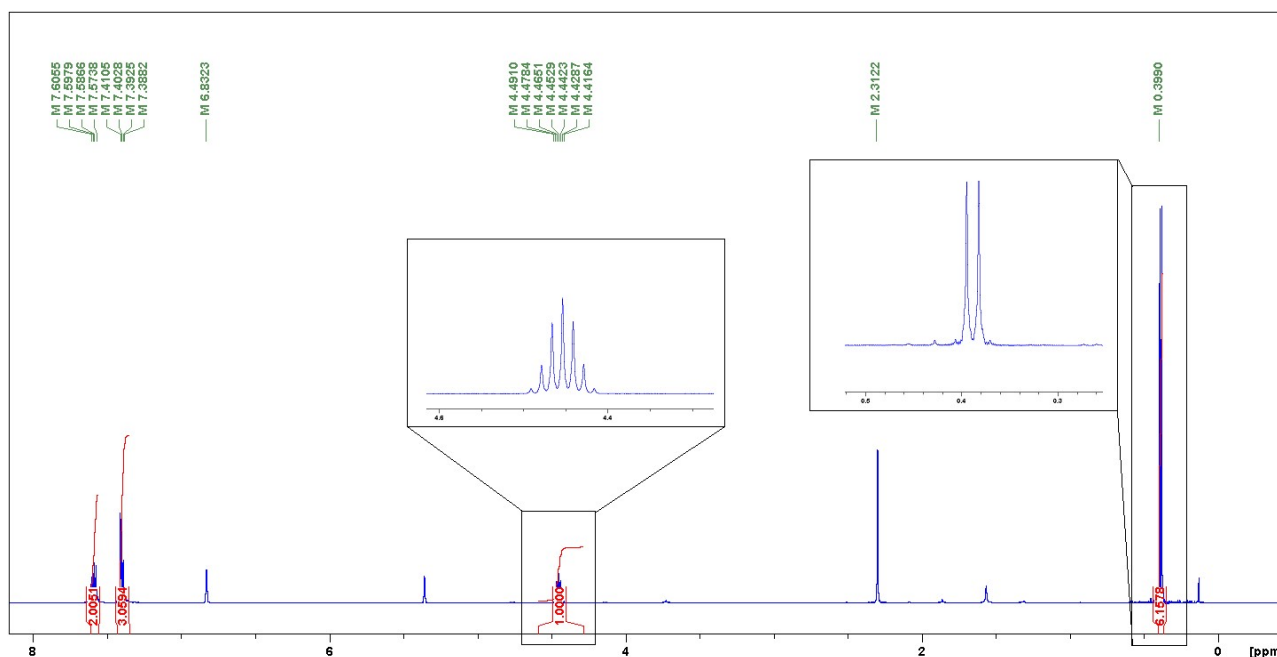


**Figure S16.** <sup>1</sup>H NMR spectrum (CD<sub>2</sub>Cl<sub>2</sub>, 300 MHz) of catalysis with [Ru(COD)(COT)].

## S6. NMR and HRMS data for catalytic reactions products.

### Me<sub>2</sub>PhSiOH (2a)

Spectroscopic data for this product agree to those previously reported.<sup>6</sup>

<sup>1</sup>H NMR (400 MHz, CD<sub>2</sub>Cl<sub>2</sub>):  $\delta$  7.59 (m, 2 H, 2CH<sub>Ph</sub>), 7.38 (m, 3 H, 3CH<sub>Ph</sub>), 0.36 (s, 6 H, 2 CH<sub>3</sub>).

<sup>13</sup>C {<sup>1</sup>H} NMR (101 MHz, CD<sub>2</sub>Cl<sub>2</sub>):  $\delta$  138.3 (C<sub>qPh</sub>), 133.4, 132.9, 129.3 (2:1:2, CH<sub>Ph</sub>), -2.1 (CH<sub>3</sub>).

### (Me<sub>2</sub>PhSi)<sub>2</sub>O (3a)

Spectroscopic data for this product agree to those previously reported.<sup>6</sup>

<sup>1</sup>H NMR (400 MHz, CD<sub>2</sub>Cl<sub>2</sub>):  $\delta$  7.61 (m, 4H, 4 CH<sub>Ph</sub>), 7.39 (m, 4H, 4 CH<sub>Ph</sub>), 7.38 (m, 2H, 4 CH<sub>Ph</sub>), 0.40 (s, 12H, 6 CH<sub>3</sub>).

<sup>13</sup>C {<sup>1</sup>H} NMR (101 MHz, CD<sub>2</sub>Cl<sub>2</sub>):  $\delta$  139.8 (C<sub>qPh</sub>), 133.1, 129.3, 127.7 (2:1:2, CH<sub>Ph</sub>), 0.62 (CH<sub>3</sub>).

HRMS (CI): *m/z* calcd for C<sub>16</sub>H<sub>22</sub>NaOSi<sub>2</sub> [(*M*+Na)<sup>+</sup>]: 309.1107; found: 309.1100.

### MePh<sub>2</sub>SiOH (2b)

Spectroscopic data for this product agree to those previously reported.<sup>6</sup>

<sup>1</sup>H NMR (400 MHz, CD<sub>2</sub>Cl<sub>2</sub>): δ 7.54 (m, 4H, 4 CH<sub>Ph</sub>), 7.39 (m, 2H, 2 CH<sub>Ph</sub>), 7.33 (m, 4H, 4 CH<sub>Ph</sub>), 0.6 (s, 3H, CH<sub>3</sub>).

<sup>13</sup>C {<sup>1</sup>H} NMR (101 MHz, CD<sub>2</sub>Cl<sub>2</sub>): δ 137.7 (2 C<sub>qPh</sub>), 134.0 (4 CH<sub>Ph</sub>), 129.7 (2 CH<sub>Ph</sub>), 127.8 (4 CH<sub>Ph</sub>), -0.74 (CH<sub>3</sub>).

HRMS (CI): *m/z* calcd. for C<sub>13</sub>H<sub>15</sub>OSi [(*M*+H)<sup>+</sup>]: 215.0892; found: 215.0887.

### [(PhCH<sub>2</sub>CH<sub>2</sub>)Me<sub>2</sub>Si]<sub>2</sub>O (3c)

<sup>1</sup>H NMR (400 MHz, CD<sub>2</sub>Cl<sub>2</sub>): δ 7.32 (m, 4H, 4 CH<sub>Ph</sub>), 7.27 (m, 4H, 4 CH<sub>Ph</sub>), 7.20 (m, 2H, CH<sub>Ph</sub>) 2.71 (t, <sup>3</sup>J<sub>HH</sub> = 9.1 Hz, 4H, 2 PhCH<sub>2</sub>CH<sub>2</sub>Si), 0.96 (t, <sup>3</sup>J<sub>HH</sub> = 9.1 Hz, 4H, 2 PhCH<sub>2</sub>CH<sub>2</sub>Si), 0.17 (s, 12H, 4 CH<sub>3</sub>).

<sup>13</sup>C {<sup>1</sup>H} NMR (101 MHz, CD<sub>2</sub>Cl<sub>2</sub>): δ 145.3 (2 C<sub>qPh</sub>), 128.2, 127.7, 125.4 (2:2:1, 10 CH<sub>Ph</sub>), 29.4 (2 PhCH<sub>2</sub>CH<sub>2</sub>Si), 20.4 (2 PhCH<sub>2</sub>CH<sub>2</sub>Si), 0.04 (4 CH<sub>3</sub>).

HRMS (CI): *m/z* calcd. for C<sub>20</sub>H<sub>30</sub>NaOSi<sub>2</sub> [(*M*+Na)<sup>+</sup>]: 365,1733; found: 365,1724.

### <sup>n</sup>Pr<sub>3</sub>SiOH (2d)

Spectroscopic data for this product agree to those previously reported.<sup>7</sup>

<sup>1</sup>H NMR (400 MHz, CD<sub>2</sub>Cl<sub>2</sub>): δ 1.42 (m, 6H, 3 CH<sub>2</sub>), 1.00 (m, 9H, 3 CH<sub>3</sub>), 0.62 (m, 6H, 3CH<sub>2</sub>).

<sup>13</sup>C {<sup>1</sup>H} NMR (101 MHz, CD<sub>2</sub>Cl<sub>2</sub>): δ 18.0 (3 CH<sub>2</sub>), 17.76 (3 CH<sub>2</sub>), 16.6 (3 CH<sub>3</sub>).

HRMS (CI): *m/z* calcd. for C<sub>9</sub>H<sub>23</sub>OSi [(*M*+H)<sup>+</sup>]: 175.1518; found: 175.1509.

### <sup>n</sup>Pr<sub>3</sub>Si)<sub>2</sub>O (3d)

<sup>1</sup>H NMR (400 MHz, CD<sub>2</sub>Cl<sub>2</sub>): δ 1.36 (m, 12H, 6 CH<sub>2</sub>), 0.96 (m, 18H, 6 CH<sub>3</sub>), 0.53 (m, 12H, 6 CH<sub>2</sub>);

<sup>13</sup>C {<sup>1</sup>H} NMR (101 MHz, CD<sub>2</sub>Cl<sub>2</sub>): δ 18.5 (6 CH<sub>2</sub>), 18.2 (6 CH<sub>2</sub>), 16.8 (6 CH<sub>3</sub>).

HRMS (CI): *m/z* calcd. for C<sub>18</sub>H<sub>43</sub>OSi<sub>2</sub> [(*M*+H)<sup>+</sup>]: 331.2852; found: 331.2841.

### (EtO)<sub>3</sub>SiOH (2f)

Spectroscopic data for this product agree to those previously reported.<sup>8</sup>

<sup>1</sup>H NMR (400 MHz, CD<sub>2</sub>Cl<sub>2</sub>): δ 3.82 (q, <sup>3</sup>J<sub>HH</sub> = 7.0 Hz, 6H, 3 CH<sub>2</sub>), 1.25 (t, <sup>3</sup>J<sub>HH</sub> = 7.0 Hz, 9H, 3 CH<sub>3</sub>).

<sup>13</sup>C {<sup>1</sup>H} NMR (101 MHz, CD<sub>2</sub>Cl<sub>2</sub>): δ 59.0 (3 CH<sub>2</sub>), 18.6 (3 CH<sub>3</sub>).

HRMS (CI): *m/z* calcd. for C<sub>6</sub>H<sub>17</sub>O<sub>4</sub>Si [(*M*+H)<sup>+</sup>]: 181.0896; found: 181.0888.

### [(EtO)<sub>3</sub>Si]<sub>2</sub>O (3f)

Spectroscopic data for this product agree to those previously reported.<sup>9</sup>

<sup>1</sup>H NMR (400 MHz, CD<sub>2</sub>Cl<sub>2</sub>): δ 3.82 (q, <sup>3</sup>J<sub>HH</sub> = 7.0 Hz, 12H, 6 CH<sub>2</sub>), 1.22 (t, <sup>3</sup>J<sub>HH</sub> = 7.0 Hz, 18H, 6 CH<sub>3</sub>).

<sup>13</sup>C{<sup>1</sup>H} NMR (101 MHz, CD<sub>2</sub>Cl<sub>2</sub>): δ 59.0 (6 CH<sub>2</sub>), 17.9 (6 CH<sub>3</sub>).

HRMS (CI): *m/z* calcd. for C<sub>12</sub>H<sub>31</sub>NaO<sub>7</sub>Si<sub>2</sub> [(*M*+Na)<sup>+</sup>]: 365.1428; found: 365.1418.

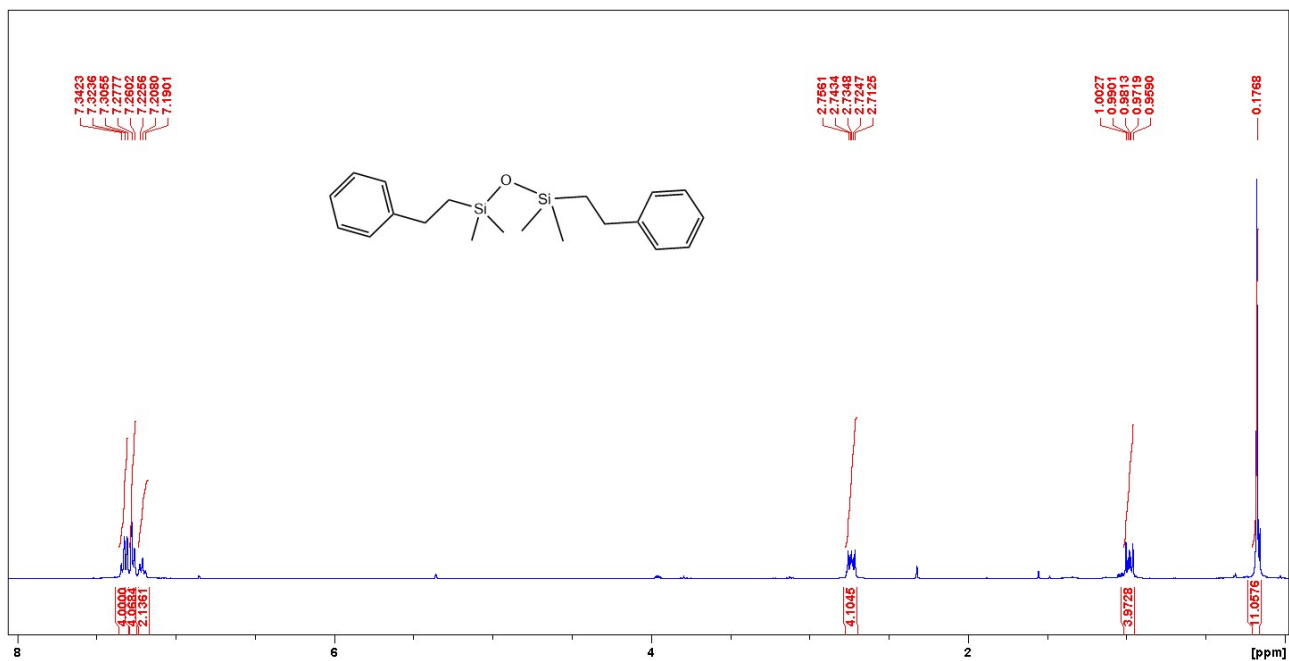


**Figure S17.** <sup>1</sup>H NMR spectrum (CD<sub>2</sub>Cl<sub>2</sub>, 400 MHz) of [(PhCH<sub>2</sub>CH<sub>2</sub>)Me<sub>2</sub>Si]<sub>2</sub>O (3c).

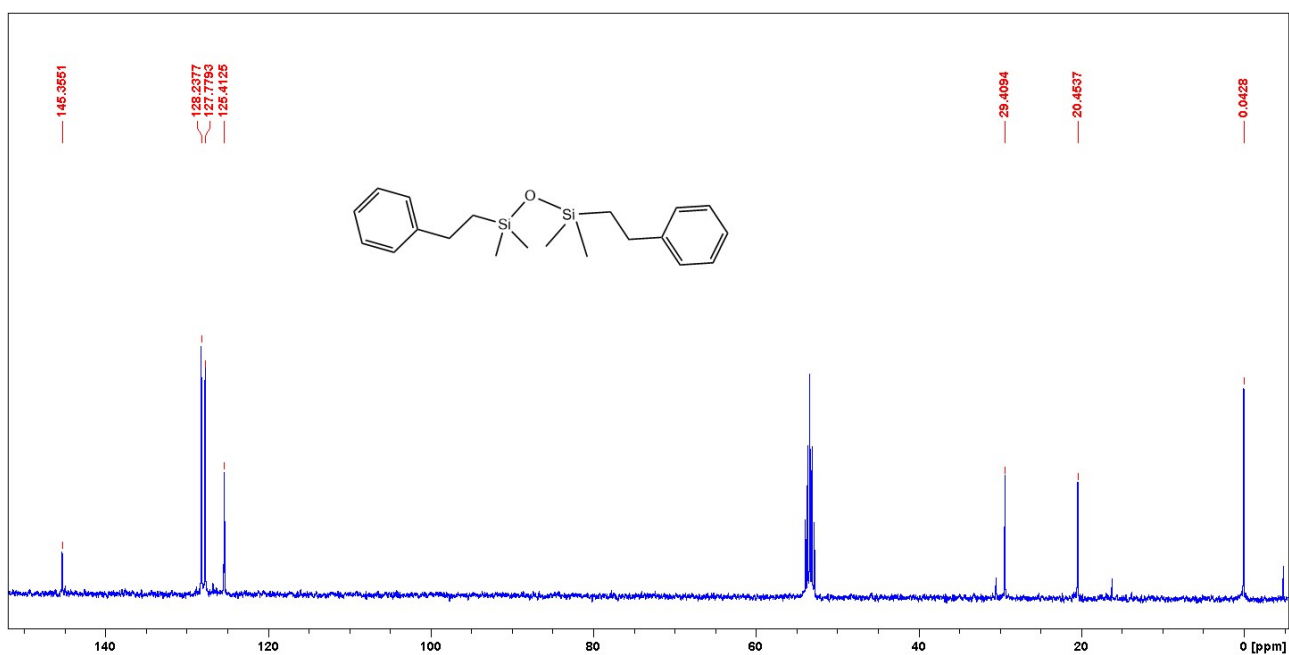


**Figure S18.** <sup>13</sup>C{<sup>1</sup>H} NMR spectrum (CD<sub>2</sub>Cl<sub>2</sub>, 101 MHz) of [(PhCH<sub>2</sub>CH<sub>2</sub>)Me<sub>2</sub>Si]<sub>2</sub>O (3c).

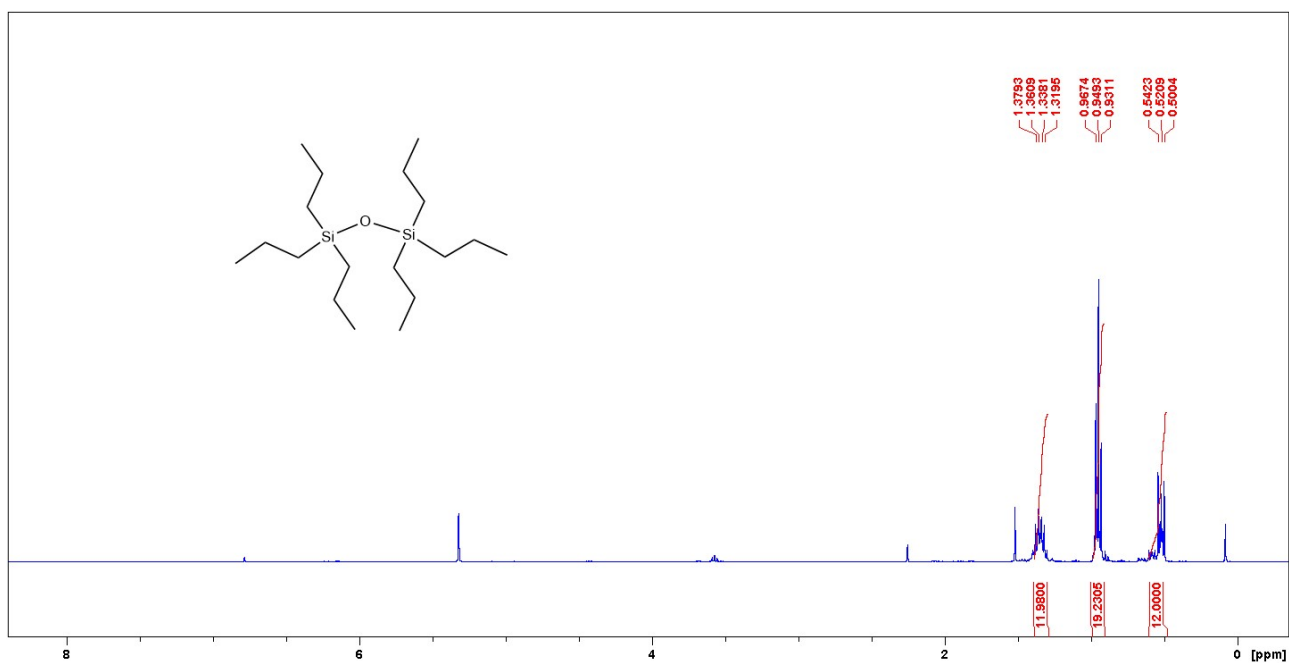


**Figure S19.**  $^1\text{H}$  NMR spectrum (CD $_2$ Cl $_2$ , 400 MHz) of  $(n\text{Pr}_3\text{Si})_2\text{O}$  (3d).

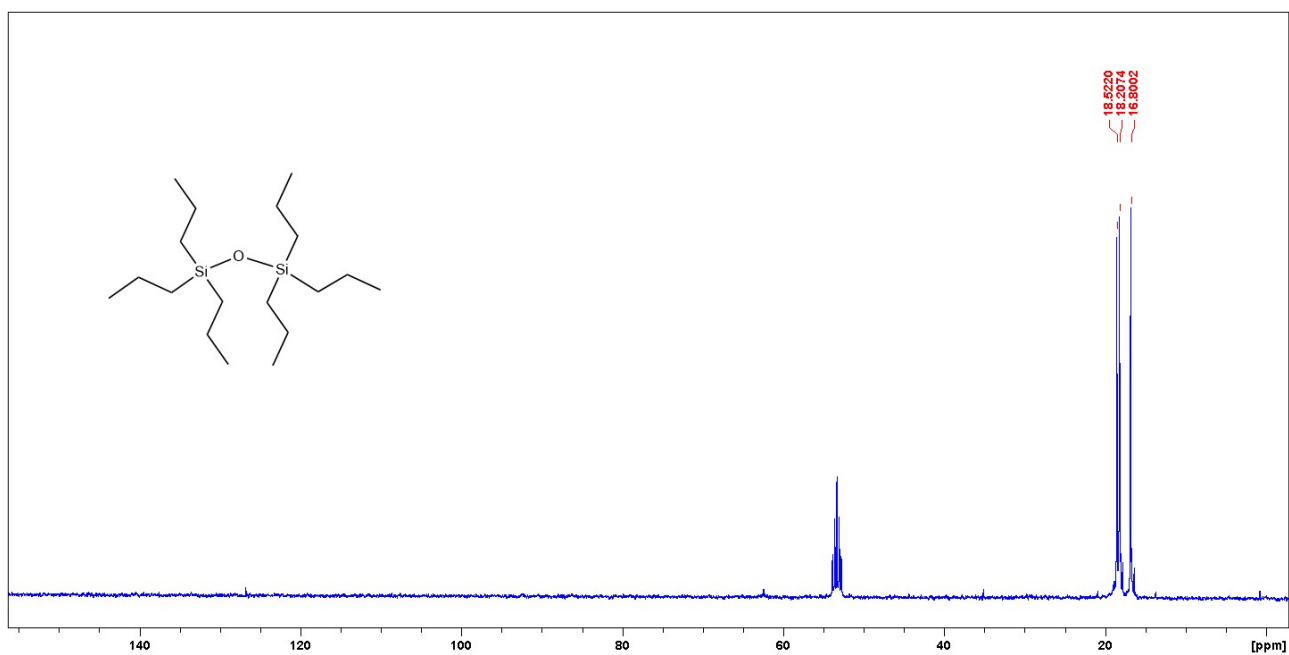


**Figure S20.**  $^{13}\text{C}\{^1\text{H}\}$  NMR spectrum (CD $_2$ Cl $_2$ , 101 MHz) of  $(n\text{Pr}_3\text{Si})_2\text{O}$  (3d).

## S7. References.

- <sup>1</sup> J. Schörghumer, A. Zimmermann and M. Waser, *Org. Process Res. Dev.* 2018, **22**, 862.
- <sup>2</sup> C. Pertuci and G. Vituli, *Inorg. Synt.* 1983, **22**, 178.
- <sup>3</sup> M. Ito, M. Itazaki, T. Abe and H. Nakazawa, *Chem. Lett.* 2016, **45**, 1434.
- <sup>4</sup> R. Kilaas, *J. Microsc.* 1998, **190**, 45-51.
- <sup>5</sup> P. Laoharajanaphand, T. J. Lin and J. O. Stoffer, *J. Appl. Polym. Sci.* 1990, **40**, 369.
- <sup>6</sup> R. Zeng, M. Feller, Y. Ben-David and D. Milstein, *J. Am. Chem. Soc.* 2017, **139**, 5720.
- <sup>7</sup> K. Shimizu, K. Shimura, N. Imaiida and A. Satsuma, *J. Mol. Catal. A: Chemical* 2012, **365**, 50.
- <sup>8</sup> V. Kazakova, O. B. Gorbatshevich and A. M. Muzafarov, *Russ. Chem. Bull.* 2005, **54**, 1350.
- <sup>9</sup> N. Ueda, T. Gunji and Y. Abe, *J. Sol-Gel Sci. Technol.* 2008, **48**, 163.